Noninvasive in vivo imaging of CD4 cells in simian-human immunodeficiency virus (SHIV)–infected nonhuman primates

Michele Di Mascio,[1] Chang H. Paik,[2] Jorge A. Carrasquillo,[3] Jin-Soo Maeng,[2] Beom-Su Jang,[2] In Soo Shin,[2] Sharat Srinivasula,[4] Russ Byrum,[5] Achilles Neria,[2] William Kopp,[6] Marta Catalfamo,[1] Yoshiaki Nishimura,[1] Keith Reimann,[7] Malcolm Martin,[1] and H. Clifford Lane[1]

[1]National Institute of Allergy and Infectious Diseases, National Institutes of Health (NIH), Bethesda, MD; [2]Warren G. Magnuson Clinical Center, NIH, Bethesda, MD; [3]Memorial Sloan-Kettering Cancer Center, New York, NY; [4]Biostatistics Research Branch, SAIC-Frederick Inc, National Cancer Institute (NCI)–Frederick, MD; [5]Bioqual, Rockville, MD; [6]Clinical Services Program, NCI-Frederick, MD; and [7]Beth Israel Deaconess Medical Center, Boston, MA

Since the earliest days of the HIV epidemic, the number of CD4^{+} T cells per unit volume of blood has been recognized as a major prognostic factor for the development of AIDS in persons with HIV infection. It has also been generally accepted that approximately 2% of total body lymphocytes circulate in the blood. In the present study, we have used a nondepleting humanized anti-CD4 monoclonal antibody labeled with the gamma emitter indium-111 to visualize the CD4^{+} T-cell pool in vivo in nonhuman primates with simian HIV infection. A strong correlation was noted between radiotracer uptake in spleen, tonsil, axillary lymph nodes, and peripheral blood CD4 T-cell counts ($\rho = 0.75$, 0.93, and 0.85, respectively, $P < .005$). The relationship between radiotracer retention in lymphoid tissues and CD4^{+} T-cell counts in the circulation was governed by an exponential law. These data provide an estimate for the total number of lymphocytes in the body as being between 1.9 and 2.9×10^{12} and suggest that the partition between peripheral blood and lymphoid tissue is between 0.3% and 0.5%. (Blood. 2009; 114:328-337)

Introduction

It has been generally accepted that only 2% of total body lymphocytes circulate in the blood.[1,2] Despite the importance attached to the measurement of the number of CD4^{+} T cells per unit volume of blood, a series of epidemiologic studies have determined that changes in the numbers of peripheral blood CD4^{+} T cells can only account for up to 30% of the variability in the clinical course of patients with HIV infection.[3] Current approaches to monitor CD4^{+} T-cell number in regions outside the peripheral blood require the use of invasive techniques (biopsies for certain organs or postmortem procedures for other organs) and are prone to sampling error. Little is known about the prognostic values of total body (or organ specific) CD4 T-cell depletion to progression to AIDS or failure of antiretroviral therapy. Thus, it is possible that a more precise assessment of the whole-body CD4 pool would enhance our understanding of HIV pathogenesis and response to therapy. In 1996, Rubin et al described the use of an indium-111–labeled rat anti–mouse CD4 monoclonal antibody (mAb) for radio-immunoscintigraphy determination of the CD4 lymphocytes distribution in mice.[4] To apply this approach to nonhuman primates and possibly to humans, we have used the CDR-OKT4A/hIgG4 mAb, a nondepleting humanized monoclonal antibody that binds to CD4 molecules from humans and rhesus macaques.[5] To image CD4^{+} cells throughout the body, only trace amounts of this humanized mAb are needed ($\sim$ 20 μg/kg), thus reducing the risk for toxicity or immunogenicity during longitudinal analyses in human studies.

Methods

Preparation of ^{111}In-labeled antibody

CDR-OKT4A/hIgG4 mAb was provided by Johnson & Johnson Pharmaceutical Research and Development. The mAb (molecular weight, 150 kDa) was conjugated with the A″ stereoisomer of 2-(p-isothiocyanatobenzyl)-cyclohexyl-diethylenetriaminepentaacetic acid (CHX-A″-DTPA, molecular weight, 739; Macrocyclic) as reported previously.[6,7] The resulting conjugate CHX-A″-DTPA-OKT4A/hIgG4 (for simplicity, DTPA-OKT4A/hIgG4; 125 μg) was labeled with [111]In (1.4 mCi/4 μL; PerkinElmer Life and Analytical Sciences). The radiochemical purity was assessed by high performance liquid chromatography (Gilson).

CD4 cell-binding assays

A total of 10^6 MT4 cells in 50 μL phosphate-buffered saline (PBS) containing 1% bovine serum albumin were incubated with increasing concentrations of OKT4A/hIgG4 or DTPA-OKT4A/hIgG4 ranging from 0.055 pM to 55 nM at 4°C for 30 minutes. After washing with 2 mL of cold PBS, cells were resuspended in 50 μL PBS and incubated for 30 minutes with a secondary mAb (donkey F(ab′)$_2$ fragment donkey anti–human IgG, Jackson ImmunoResearch Laboratories) fluorescein isothiocyanate–conjugated for flow cytometric analysis. The binding affinity, k_d, of the modified and unmodified mAbs was obtained from antibody dilution analysis.[8] The immunoreactivity of the radiolabeled products was tested using a modification of the cell-binding assay described by Lindmo et al.[9]

CD4 cell radiotracer retention and internalization assays

The radiolabeled ^{111}In-DTPA-OKT4A/hIgG4 was added to 85×10^6 MT4 cells at a concentration of 1 ng/μL in total volume of 11 mL and incubated

Table 1. Animal subjects study design

Animal ID	Rhesus origin, sex	SHIV strain	Duration of infection, years	CD4 T cells*	CD8 T cells*	CD20 cells*	SHIV-RNA† copies/mL	Injected dose infusion, mCi	Imaging time pri,‡ hours
RH598	Indian, male	89.6P	6.5	2314	2820	129	< 110	1.55	48
CH3397	Chinese, female	Uninfected	NA	1700	2641	868	NA	1.94	48
RH4000	Indian, male	Uninfected	NA	1672	1730	439	NA	1.69	45, 136
RH600	Indian, male	89.6P	6.5	1408	2295	990	< 110	1.34	48
RH637	Indian, male	89.6P	6.5	625	1719	187	< 110	1.90	48
RH638	Indian, male	89.6P	6.5	604	2000	124	< 110	2.04	48
RH651	Indian, male	89.6P	6.5	423	745	221	< 110	1.37	48
RH4019	Indian, male	DH12R	0.4	194	979	477	< 110	1.60	48
RH4001	Indian, male	DH12R	0.4	71	2460	540	8310	1.67	48
RHCL6G	Indian, male	DH12R	1	50	1213	203	7620	1.45	1, 45, 136
RH4021	Indian, male	DH12R	0.4	5	811	313	25 093	1.38	48

A total of 11 adult monkeys were imaged (median age, 7 years, range, 7-11 years; median weight, 11.3 kg, range, 8.6-15 kg). One uninfected female Chinese rhesus macaque (CH3397), 1 uninfected male Indian rhesus macaque (RH4000), 5 male SHIV$_{89.6P}$-infected Indian rhesus macaques (RH598, RH600, RH637, RH638, and RH651), and 4 SHIV$_{DH12R}$-infected (RH4019, RH4001, RHCL6G, and RH4021) Indian rhesus macaques were recruited in this study from 2 completed studies at the National Institutes of Health (NIH). The 5 SHIV$_{89.6P}$-infected rhesus macaques were selected for the CD4 T-cell counts from a group of rhesus macaques that had been immunized with 2×10^8 infectious units of recombinant modified vaccinia virus Ankara MVA/KB9 as part of another study[12] and challenged intrarectally with 20 infectious units of SHIV$_{89.6P}$. These macaques showed complete control of viral load and high levels of CD4 cell counts after the phase of acute infection after intrarectal viral inoculation. The 4 SHIV$_{DH12R}$-infected rhesus macaques were challenged with 1.85×10^6 TCID50 SHIV$_{DH12R}$ clone-7. Three of these 4 animals were treated with an experimental antiretroviral drug during the first 2 weeks after the viral inoculation, as part of another study (T. Igarashi, Y.N., M.M., unpublished observations, February, 2007), which led to partial control of viral replication during the chronic phase of the infection. To identify the optimal timing of imaging, 2 animals (RH4000 and RHCL6G), with high and low CD4 T-cell counts, respectively, were imaged at 1, 45, and 136 hours postradiotracer injection (pri) with SPECT encompassing 3 different fields of view (skull, abdomen, and pelvis). Based on these images, the optimal imaging time for the visualization of lymphoid organs was defined at approximately 48 hours pri for the other animals (data not shown), and all subsequent imaging was done at this time.

NA indicates not applicable.

*Cells/μ L at the time of imaging.

†SHIV viremia at the time of imaging.

‡Imaging time postradiotracer injection (pri)

at 4°C for 90 minutes. After the 90-minute incubation, the cells were washed twice with cold PBS to remove the unbound radioactivity and replated at a ratio of 10^6 MT4 cells per 1 mL RPMI 1640 medium, warmed at 37°C in a humidified 5% CO_2 incubator. Aliquots containing 10^6 labeled cells were collected at 1, 2.5, 3.5, 5, and 17 hours. At each collection, cells were washed twice and the percentage of ^{111}In-DTPA- OKT4A/hIgG4 bound to cells was determined in a gamma counter. The internalized cell-associated fraction was determined with an acid wash method.[10,11]

Animal subject study design

An outline of the protocol design and the number of adult monkeys imaged are shown in Table 1.[12] All animals used in this study were maintained in accordance with the *Guide for the Care and Use of Laboratory Animals*.[13] They were housed in a biosafety level 2 facility; biosafety level 3 practices were followed. Phlebotomies and virus inoculation were performed with animals anesthetized with ketamine/acepromazine.

Imaging and biodistribution studies

The animal studies were performed under a protocol approved by the National Institutes of Health (NIH) Institutional Animal Care and Use Committee. The animals were anesthetized with ketamine (10 mg/kg) and acepromazine (0.1 mg/kg). The images were obtained with a medium-energy collimator. Single photon emission computed tomography (SPECT) images were analyzed by manually drawing consecutive regions of interest over the transversal sections of the heart, liver, kidney, bone marrow, tonsils, submandibular, axillary and inguinal lymph nodes, and spleen to cover the entire volume of the organs (volume of interest [VOI]). The retention of radiotracer for each VOI was obtained from the maximum activity in the VOI minus the background activity in a VOI placed close to the organ, and normalized on the maximum activity in the liver. The retention of radiotracer was also calculated as an index of the quantitative standardized uptake value,

$$I_{SUV} = \frac{C}{ID} w$$

where *C* is the maximum counts in the VOI and *ID* and *w* are the injected dose (expressed in mCi) and body weight, respectively.

Ex vivo biodistribution study

The ex vivo biodistribution of the ^{111}In-DTPA-OKT4A/hIgG4 was assessed in CH3397, RH637, and RH638 soon after the SPECT imaging; and at a later time point (after a new radiotracer injection ∼ 5 months after the imaging time point) for RH600 (CD4$^+$ T cells = 1836/μL), RH4019 (CD4$^+$ T cells = 239/μL), RH4001 (CD4$^+$ T cells = 39/μL), and RHCL6G (CD4$^+$ T cells = 24/μL). These 7 animal subjects were sacrificed approximately 48 hours after radiotracer injection and small aliquots of organs (submandibular, axillary, inguinal and mesenteric lymph nodes, tonsils, spleen, lung, kidney, liver, jejunum, ileum, ascending and descending colon) were weighed and counted in the gamma counter. Undigested waste products of intraluminal gut subcompartments were removed and the tissue rinsed clean with PBS. The retention of radiotracer in each organ was obtained by normalizing the activity expressed as counts per minute (cpm) per unit mass (g) in that organ on the activity per unit mass in the liver. One animal (RH600) was eliminated from this analysis because of lack of measurement of liver uptake of the radiotracer. For one animal (RH4001), the liver uptake was not available from measurements obtained with the gamma counter, and was estimated from an additional SPECT imaging obtained immediately prior to the sacrifice of the animal.

Cell extraction from tissues and CD4$^+$ purification

Lymph nodes, tonsils, and spleen were mechanically disrupted by pressing through a 70-μm pore size cell strainer (Fisher Scientific). Aliquots of organs from the small and large intestine representing a mixture of lymphoid tissues, including lamina propria, lymphoid nodules, and Peyer patches, were first digested using 0.5 mg collagenase (Sigma-Aldrich) for 30 minutes at 37°C before being filtered through a 70-μm screen. Erythrocytes were lysed with ACK lysing buffer (Lonza Walkersville), and cells were washed with complete RPMI medium. Cells were stained with trypan blue to obtain the number of total viable cells. The radioactivity of the collected cells resuspended in 1 mL PBS was recounted in the gamma counter. For some tissues, CD4$^+$ cells were isolated using Miltenyi MiniMACS Separator (Miltenyi Biotec). Isolated cells were resuspended in 1 mL of PBS, and the radioactivity was recounted in the gamma counter.

Tissue section staining

Immunohistochemical staining of fixed tissue of CD3^{+} and CD20^{+} cells is given in supplemental data (available on the *Blood* website; see the Supplemental Materials link at the top of the online article).

Statistical methods

The binding affinity, k_d, of the modified and unmodified mAbs was obtained by best-fitting a theoretical sigmoid curve to both set of data. The correlation between radiotracer uptake in VOIs and T-cell counts in the blood was tested with the Spearman rank correlation test (ρ). To account for the high number of tests performed, P values less than .01 were considered statistically significant. Mixed-effect linear model with multiple samples per subject was used to estimate the parameters of Equation 2.

Results

Radiolabeling and specificity of binding of the radiotracer

To label the OKT4A/hIgG4 with ^{111}In, the mAb was conjugated with DTPA derivative, the A″ stereoisomer of 2-(*p*-isothiocyanato-benzyl)-cyclohexyl-DTPA. The specific binding of the conjugated and unconjugated mAbs to MT4 cells was tested by flow cytometry. No statistically significant difference was observed between the estimates of k_d for DTPA-OKT4A/hIgG4 (0.22 nM, 95% confidence interval [CI], 0.18-0.28) and OKT4A/hIgG4 (0.29 nM, 95% CI, 0.20-0.39, P = .41), confirming that conjugation did not modify the binding affinity of the mAb to CD4 molecules (Figure 1A). The mean fluorescence intensity of stained MT4 cells was also unchanged between the 2 antibodies (data not shown). ^{111}In-DTPA-OKT4A/hIgG4 was determined to be stable in serum for a 5-day period at 37°C, and there were no ^{111}In-transferrin or smaller molecular ^{111}In-catabolites detected when serum samples were analyzed by size exclusion high performance liquid chromatography (data not shown). The retained specific binding of the ^{111}In-radiolabeled products was demonstrated in MT4 cells using a modification of the saturation cell-binding assay under antigen excess conditions using the method of Lindmo and Bunn.[9] Binding inhibition with excess amounts of the cold mAb was approximately 99% of the total incubated radioactivity and was independent of the concentration of radiotracer, suggesting that the radioactivity trapped in the cell pellet of MT4 cells was the result of specific binding of the ^{111}In-DTPA-OKT4A/hIgG4 (data not shown). The percentage of the labeled mAb bound to cells was approximately 60% at 4×10^6 MT4 cells, and its immunoreactivity was estimated to be approximately 100% extrapolated under condition of excess receptors concentration (not shown) based on the Lindmo method[9] (Figure 1B). As shown in Figure 1C, the ^{111}In cell-associated radioactivity decreased by approximately 10% after 3.5 hours at 37°C and an additional 10% after 13.5 hours at 37°C. Before incubation at 37°C, approximately 65% of the cell-associated radioactivity was removable with an acid solution and therefore on the cell surface (Figure 1C). Thus, the percentage of internalized radiotracer increased up to 74% at 17 hours.

To image CD4^{+} cells in vivo, monkeys received 1.63 plus or minus 0.24 mCi of ^{111}In-DTPA-OKT4A/hIgG4 intravenously after fasting for at least 8 hours. A summary of the imaging experiments and characterizations of the monkeys imaged are shown in Table 1. No association was found between the mean fluorescence intensity of CD4 T cells in the peripheral blood and the peripheral blood CD4 T-cell count (data not shown). To demonstrate the specificity of ^{111}In-DTPA-OKT4A/hIgG4 binding to CD4^{+} cells in vivo, CD4^{+} cells were isolated from the spleen and lymph nodes of

2 monkeys 48 hours after the administration of radiotracer and the total radioactivity associated with the CD4^{+} and CD4^{−} cells determined. As expected, the levels of the radiotracer associated with the CD4^{+} cells were consistently higher than the levels of the radiotracer in the CD4^{−} cells (mean ratio, 16.9, P = .007), thus showing specificity of binding to CD4^{+} cells (Figure 1D).

In vivo SPECT imaging

^{111}In-DTPA-OKT4A/hIgG4 whole-body and SPECT images were acquired from the top of the skull to the inguinal region for all animals. The time-activity curve of the radiotracer at 1, 45, and 136 hours after radiotracer injection was obtained in 2 animals (Figure 2A). The radiotracer accumulated primarily in the liver and, to a smaller extent, in the kidneys (Figure 2A-C), consistent with biodistribution studies of other ^{111}In-labeled mAbs in mice[4,6] or humans.[14,15] No differences in radiotracer accumulation in these 2 organs were noted between monkeys with different peripheral blood CD4^{+} T-cell counts, suggesting that the hepatic uptake of the radiotracer was the result of nonspecific retention. Uptake of radiotracer was also noted in tonsils, submandibular, axillary and inguinal lymph nodes, and the spleen, as is shown for the uninfected female monkey (CH3397; Figure 2B). In contrast to liver and renal uptake, monkeys with higher CD4^{+} T-cell counts ($> 1400/\mu L$) showed a higher uptake of radiotracer in lymph nodes, tonsils, and spleen with the greatest uptake in the spleen. The 3 monkeys with the lowest CD4^{+} T-cell counts ($< 100/\mu L$) showed little to no activity in the same tissues. The animals with intermediate levels of CD4^{+} T-cell counts (100-$1400/\mu L$) showed a well-defined spleen but less uptake in lymph nodes or tonsils (Figure 2C-D). The evidence of an association between the level of uptake of the radiotracer in these lymphoid organs and the peripheral blood CD4^{+} T-cell count suggests that the uptake of the radiotracer in these organs is mostly explained by its specific binding to CD4^{+} cells.

The presence of small amounts of radiotracer in the gastrointestinal tracts was similar in the 3 groups of animals consistent with the intraluminal activity observed with other ^{111}In-labeled antibodies.[14] As confirmed from the direct measurements of radioactivity in these organs at necropsy, the activity observed in the gut compartments was primarily the result of nonspecific uptake of the radiotracer, consistent with imaging data of ^{111}In-labeled anti-CD4 mAb from normal mice.[4,16]

Semiquantitative measurements of radioactivity from different organs were obtained from the SPECT images by dividing the maximum pixel counts of the VOI by the maximum pixel counts of the liver. Regardless of CD4^{+} T-cell count, no differences in image intensity were observed for the liver or for the retention of radiotracer in the kidney, bone marrow, or testes. In contrast, strong correlations were noted between the radiotracer retention in lymphoid tissues and peripheral blood CD4^{+} T-cell count (Figure 3A-B). The highest Spearman rank correlations were noted for the tonsil (ρ = 0.93, $P < .001$), axillary lymph nodes (ρ = 0.85, $P < .001$), and spleen (ρ = 0.75, P = .004). A trend toward lower retentions of the radiotracer in animals with lower peripheral blood CD4^{+} T-cell counts was also observed in the submandibular, inguinal lymph nodes, and the heart (the latter perhaps related to the presence of bronchial-mediastinal lymph nodes), although these correlations did not achieve statistical significance. No significant correlations were observed between the retention of radiotracer and CD8^{+} T cell or CD20^{+} (B) cell counts (data not shown). Similar conclusions derived from calculating the relative
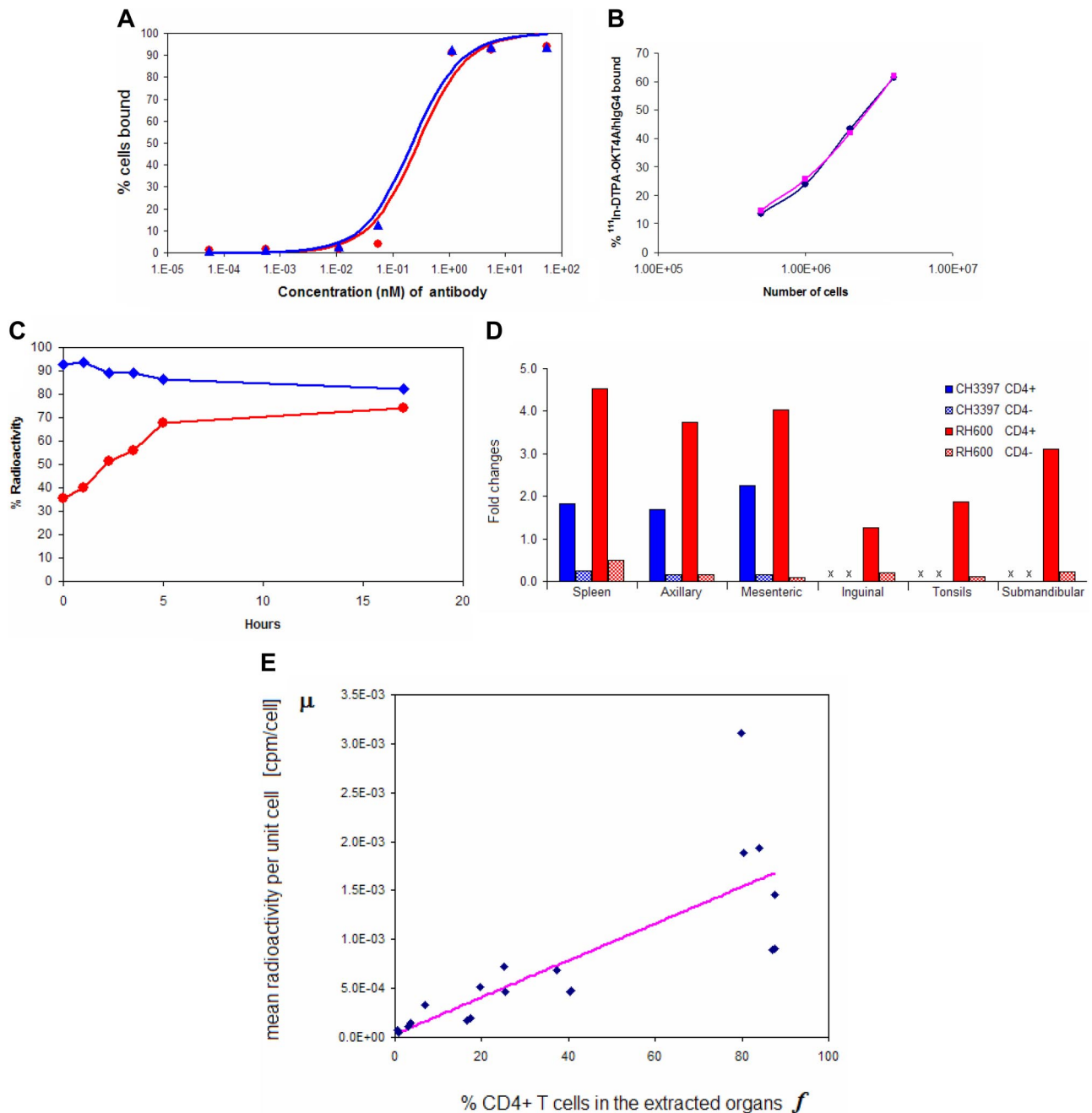
Figure 1. Binding affinity and immunoreactivity of OKT4A/hIgG4 and ^{111}In-DTPA- OKT4A/hIgG4 to MT4 cells. (A) Assay based on constant cell concentration. Percentage of cells-bound mAb was plotted vs increasing concentrations of OKT4A/hIgG4 (red circles) or DTPA-OKT4A/hIgG4 (blue triangles) mAb. (B) Assay based on constant ^{111}In-DTPA-OKT4A/hIgG4 concentration. The percentage of ^{111}In-DTPA-OKT4A/hIgG4 bound to MT4 cells was plotted vs the number of MT4 cells. The specific activity of the labeled antibody was more than 11 mCi/mg. The labeled antibody with a radiochemical purity of more than 98% was used for the cell-binding and the imaging studies. (C) The radiotracer retention and internalization assays were performed in MT4 cells warmed at 37°C in a humidified 5% CO_2 incubator. The percentage of ^{111}In-DTPA-OKT4A/hIgG4 bound to MT4 cells (blue) was obtained by dividing the radioactivity associated with cell pellets by the total radioactivity measured in 1-mL aliquots of cells suspensions; the internalized cell-associated fraction was determined with an acid wash method[10,11] (red). (D) Ratios (fold changes) of the cpm/CD4$^+$ over cpm/cell and cpm/CD4$^-$ over cpm/cell. Extracted total cell suspensions were obtained from spleen and lymph nodes of CH3397 and RH600 after lysing erythrocytes, and the total cell pellet counted in the gamma counter. CD4$^+$ cells were isolated with magnetic beads and the total radioactivity associated with the CD4$^+$ and CD4$^-$ cells determined (expressed as cpm). Ratios (fold changes) of the cpm/CD4$^+$ over cpm/cell and cpm/CD4$^-$ over cpm/cell are shown for positive and negative selections of cells purified with magnetic beads from organs extracted from CH3397 and RH600. x indicates not available. (E) Best fit to the linear model in Equation 2 of the data collected from unpurified, positive and negative selections of cells extracted from organs of RH600.

index of standardized uptake value, I_{SUV} ("Imaging and biodistribution studies") with the highest correlations between this variable and the peripheral blood CD4$^+$ T-cell count observed in the spleen ($\rho = 0.86$, $P < .001$), axillary lymph nodes ($\rho = 0.83$, $P < .001$), and tonsils ($\rho = 0.82$, $P = .001$) and no statistically significant correlations observed in the other organs. Similarly, no statistically

significant correlations were observed between I_{SUV} and CD8$^+$ T-cell or CD20$^+$ (B) cell counts (data not shown).

The relationship between the CD4$^+$ T-cell count in the peripheral blood and the retention of radiotracer in lymphoid tissues was found to be nonlinear. This nonlinear relationship appears to be well described by an exponential law as shown in Figure 3C for the spleen and the tonsils.
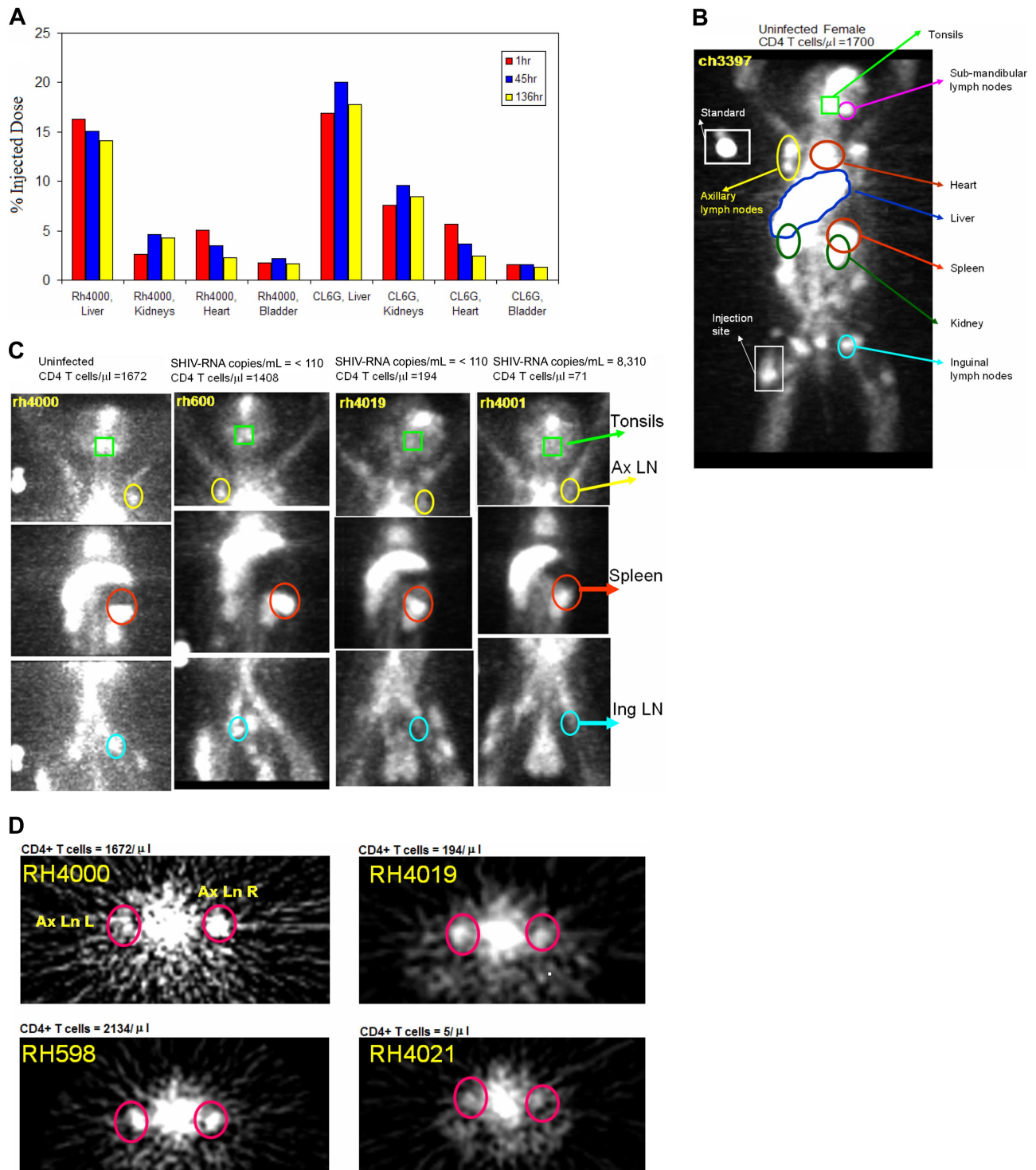
Figure 2. Trans-SPECT images of monkeys with different CD4 T-cell counts. The total amount of injected DTPA-OKT4A/hIgG4 for each monkey was approximately 200 μg. (A) Time-activity curves of the radiotracer for the liver, kidneys, heart, and bladder at 1, 45, and 136 hours after radiotracer injection obtained from the whole-body images acquired in the uninfected RH4000 and the simian HIV$_{DH12R}$-infected RHCL6G. (B) Trans-SPECT total body image of the uninfected female CH3397. (C) Trans-SPECT sections of 4 monkeys. Spleen, tonsils, and axillary and inguinal lymph nodes regions of interest are circled. (D) Transversal sections of 4 monkeys. Right and left axillary lymph nodes are circled. The radioactivity in the middle is heart blood pool.

The same nonlinear trend was observed in the spleen, tonsils, and lymph nodes when the retention of radiotracer was replaced by the index of standardized uptake value, I_{SUV} (data not shown).

Ex vivo biodistribution study

Direct measurements of radioactivity of excised organs from 6 monkeys were used to validate the distribution of the radiotracer obtained from imaging data. Similar to what was observed in the whole-body imaging studies, the radioactivity measurement of individual organs revealed no differences between animals with high and low CD4 T-cell counts, in radiotracer uptake in lung, kidney, whole blood, or any subcompartments (jejunum, ileum, ascending and descending colon) of the small and large intestine. In
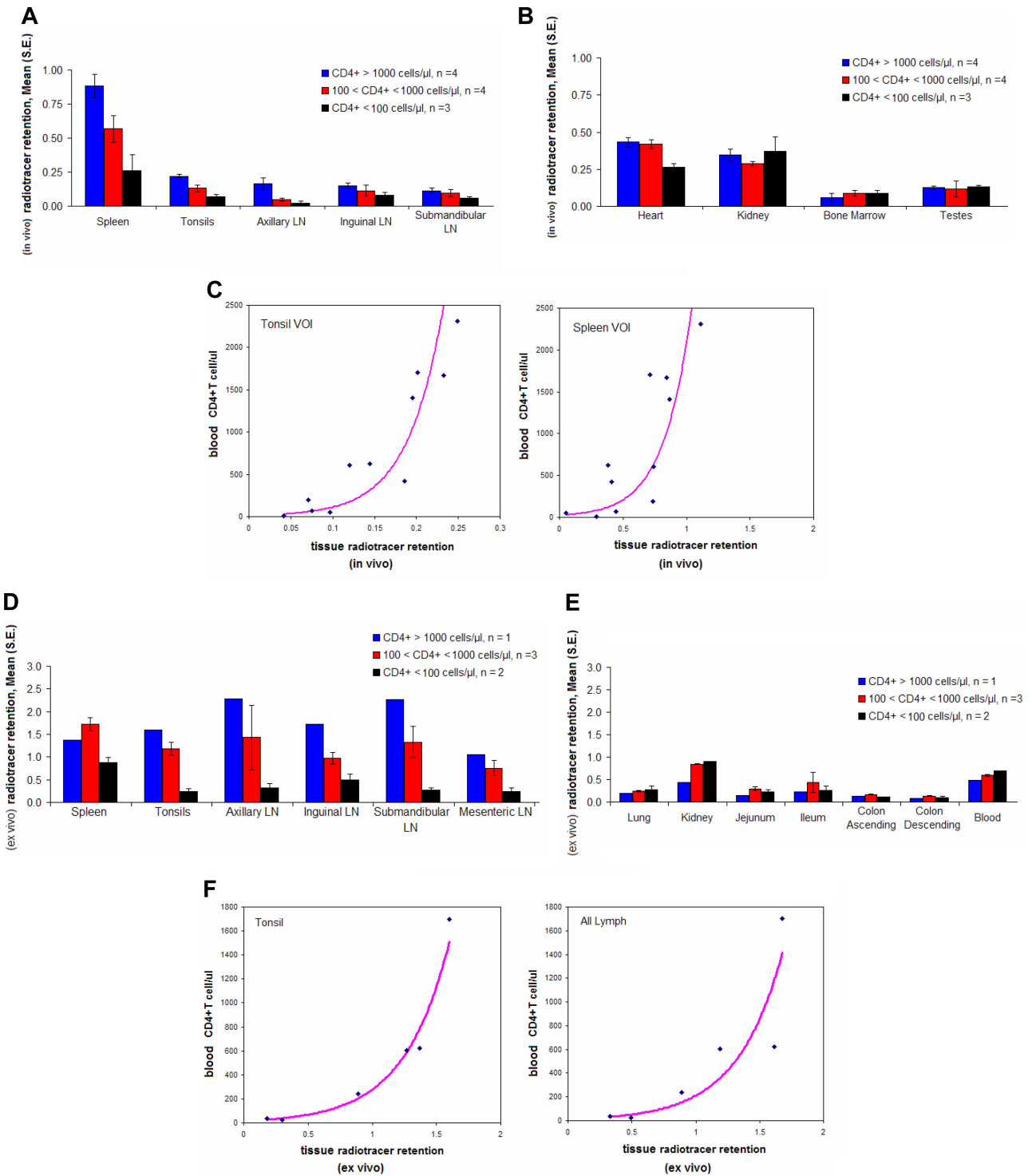
Figure 3. Three-dimensional semiquantitative analysis of SPECT images and ex vivo biodistribution study. Monkeys were grouped in high (blue bars), intermediate (red bars), and low (black bars) peripheral blood CD4 T-cell counts. The radiotracer retention from imaging data was calculated. For each VOI, the maximum pixel activity of radiotracer uptake was obtained and values were normalized on the maximum activity in the liver. (A) Mean ($\pm$ SE) of normalized maximal counts in spleen, lymph nodes, and tonsils. (B) Mean ($\pm$ SE) of normalized max counts in heart, kidney, bone marrow, and testes. (C) Relationship between CD4 T-cell counts in the peripheral blood and retention of ^{111}In-DTPA-OKT4A/hIgG4 estimated from imaging data in tonsils and spleen VOIs. R^2 for the fit of the exponential model to the data observed in the tonsils ($R^2 = 0.77$, $P < .001$, n = 11); in the spleen ($R^2 = 0.56$, $P = .008$, n = 11). (D) The radiotracer retention from organs collected from 6 monkeys was derived from the counts per minute normalized on the mass (cpm/g) of each organ divided by the cpm/g of the liver, for both lymphoid organs and (E) for lung, kidney, blood, and subcompartments of small and large intestine (radiotracer retention for kidney and blood of RH4001 (CD4$^+$ T cells = 39/μL), not available). (F) Relationship between CD4 T-cell counts in the peripheral blood and retention of ^{111}In-DTPA-OKT4A/hIgG4 estimated from ex vivo data in tonsils and mean value of all lymphoid organs analyzed (spleen, tonsils, submandibular, axillary, inguinal, and mesenteric lymph nodes).

contrast, the retention of radiotracer was lower in the lymphoid organs (spleen, tonsils, axillary, inguinal, submandibular, and mesenteric lymph nodes) in the animals with lower peripheral

blood CD4 T-cell counts compared with those with higher peripheral blood CD4 T-cell counts (Figure 3D-E). High correlations were noted between the retention of radiotracer in lymphoid organs

and the peripheral blood CD4+ T-cell count ($\rho = 0.89\text{-}0.95$, $P < .01$), with the exception of the spleen ($\rho = 0.43$, $P = .198$). No significant correlations were observed between the retention of radiotracer in the blood, lung, kidneys, or any subcompartments (jejunum, ileum, ascending and descending colon) of the small and large intestine and the peripheral blood $CD4^+$ T-cell count. No significant correlations were observed between the retention of radiotracer and $CD8^+$ T- or $CD20^+$ (B) cell counts (data not shown). The relationships between the $CD4^+$ T-cell count in the peripheral blood and the retention of the radiotracer directly measured in the tonsils or all lymphoid organs ex vivo are shown in Figure 3F. As in the case of the whole-body imaging, nonlinear (exponential) relationships were observed between peripheral blood $CD4^+$ T-cell counts and tonsils ($R^2 = 0.97$, $P < .001$, n = 6) or mean value for all lymphoid organs ($R^2 = 0.89$, $P = .004$, n = 6). Based on this relationship, one could extrapolate that: (1) for a subject starting with 1000 $CD4^+$ T cells/μL in the peripheral blood, a drop to 500 cells/μL is associated with approximately a 20% decrease in the number of $CD4^+$ cells per unit mass of lymphoid tissue, whereas (2) for a subject starting with 100 $CD4^+$ T cells/μL, a decline to 50 cells/μL is associated with approximately a 45% decrease in the number of $CD4^+$ cells per unit mass of lymphoid tissue. Thus, for subjects with low $CD4^+$ T-cell counts, changes in the number of $CD4^+$ T cells in the blood predict larger changes in the number of $CD4^+$ cells per unit mass of lymphoid tissues than the changes in lymphoid tissue predicted for subjects with higher $CD4^+$ T-cell counts in the peripheral blood.

Determination of CD4 receptor occupancy 48 hours after administration of ^{111}In-DTPA-OKT4A/hIgG4

Measurements of mean radioactivity per unit cell from the unpurified cell pellet and from the $CD4^+$ and $CD4^-$ selections were used to extrapolate the receptor occupancy after administration of the radiotracer. If each $CD4^+$ cell carries p_1 mAb and each $CD4^-$ cell carries p_2 mAb, then the mean number of mAbs per cell (μ) in an organ with n_1 $CD4^+$ cells and n_2 $CD4^-$ cells is given by Equation 1

$$\frac{n_1 p_1 + n_2 p_2}{n_1 + n_2} = \mu$$

The mean number of mAbs per unit cell can be expressed as a linear function of the fraction of $CD4^+$ cells in the cell pellet Equation 2

$$f = \frac{n_1}{n_1 + n_2} : \text{Eq(2)} \quad \mu = (p_1 - p_2) f + p_2$$

A linear relationship was found between the mean radioactivity per unit cell and the fraction of $CD4^+$ cells ($r^2 = 0.69$, $P < .001$), with the fraction of $CD4^+$ cells available from flow-cytometric analysis of unpurified, positive and negative selections collected from organs extracted from RH600 (Figure 1E). From the linear fit to the data, we also estimated the mean radioactivity per unit $CD4^+$ cell to be 1.88×10^{-3} cpm/cell (95% CI, 1.57-2.19) $\times 10^{-3}$ cpm/cell), whereas the mean radioactivity per unit $CD4^-$ cell was found to be not significantly different from zero. Given the specific activity of 1.61 mCi/179 μg at the time of injection corrected for the physical half-life of ^{111}In at the time of radioactivity counted, and the mean number of receptors per $CD4^+$ T cells of 80 000,[17] we estimated an occupancy of approximately 1% of CD4 receptors per unit $CD4^+$ cell during in vivo imaging.

Calculations are as follows: the specific activity (1.61 mCi/179 μg) corrected 48 hours after injection is 1.61 mCi/291 μg at the time of radioactivity count. Thus, from the equivalence 1 mCi = 2.2×10^9 disintegrations per minute (dpm), and given our calculated efficiency of ^{111}In detection from the gamma counter of 0.96 cpm/dpm, the total mass of mAb in a $CD4^+$ cells is 1.88×10^{-3} cpm $\times$ 291 μg/(1.61 $\times$ 2.2×10^9 dpm $\times$ 0.96 cpm/dpm) = 1.61×10^{-10} μg = $1.61 \times$ 10^{-10}/(molecular weight = 150 000) = 10.73×10^{-16} μmol = 10.73×10^{-22} mol; 10.73×10^{-22} mol $\times$ (Avogadro number) $6.023 \times$ 10^{23} molecules/mol = 646 molecules or approximately 1% of CD4 molecules per $CD4^+$ cell.

To examine whether the radiotracer bound to $CD4^+$ cells might have been lost during the purification procedure, we monitored the level of radioactivity bound to MT4 cells through sequential purifications. After a 17-hour incubation of MT4-labeled cells used in the kinetic study described in Figure 1C, MT4 cells had level of radioactivity 3.82×10^{-2} cpm/cell. Thus, after the first purification with magnetic beads, the cells collected from the positive selection had a level of radioactivity of 3.69×10^{-2} cpm/cell. The following purification of the positive selection showed a level of radioactivity of 3.74×10^{-2} cpm/cell, thus indicating a lack of change in cell-associated radioactivity as result of $CD4^+$ cell separation.

Number of $CD4^+$ cells per unit mass from cell suspensions

The spleen, tonsils, and lymph nodes from 2 monkeys with high $CD4^+$ T-cell peripheral blood counts (CH3397 and RH600) were harvested and the cpm/g of tissue measured with the gamma counter. The levels of radioactivity associated with the $CD4^+$ (cpm/$CD4^+$) and $CD4^-$ (cpm/$CD4^-$) cells were measured in different organs and used to estimate the number of $CD4^+$ cells per unit mass of lymph nodes and spleen (Table 2). Using the lymph nodes and tonsils of the RH600 as reference, the mean radioactivity level associated with the unpurified tissue cell extractions was $\mu = 0.53 \times 10^{-3}$ cpm/cell, whereas the mean radioactivity level associated with the purified $CD4^+$ and $CD4^-$ cells was $p_1 = 1.42 \times 10^{-3}$ cpm/cell and $p_2 = 0.084 \times 10^{-3}$ cpm/cell, respectively. Thus, the fraction of $CD4^+$ cells in these tissues, f, can be calculated from Equation 2. From this equation, we found that the mean fraction of $CD4^+$ cells expected in these organs of monkeys with high $CD4^+$ T-cell peripheral blood count, is 33.4%, extremely close to the mean fraction of $CD4^+$ T cells, 35.1%, obtained from the independent measurement provided from flow-cytometric analysis on the same tissues, thus confirming the robustness of the measurement of radioactivity associated with cells before and after the procedure of purification. This relationship also shows that the majority of $CD4^+$ cells in these tissue pellets are $CD4^+$ T cells, as confirmed from flow-cytometric analysis (%CD4+CD3$^-$ < 1%). The radioactivity measured in one unit mass of these organs is the result of both specific binding (carried by $CD4^+$ cells, ie, ~ 90% based on Equation 1 and our data) and nonspecific binding (carried by $CD4^-$ cells, the remaining 10%). Thus, the number of $CD4^+$ cells per unit mass of tissue is approximately 90% of what is estimated by simply dividing the cpm/g on the cpm/$CD4^+$. From radioactivity data of cell suspensions, we have obtained an upper estimate of 1.4×10^9 $CD4^+$ cells per gram of spleen in CH3397 and 1.0×10^9 $CD4^+$ cells per gram of spleen in RH600 (Table 2), obtained by simply dividing the cpm/g by the cpm/$CD4^+$ of each organ. Similar numbers were estimated for the lymph nodes of the same 2 animals, characterized by high CD4 cell count in the blood (mean values, 1.4×10^9 cells/g for CH3397 and 1.9×10^9 cells/g for RH600).

Table 2. Direct measurements of radioactivity in cells extracted from excised organs of CH3397 and RH600 (administered dose, 1.94 mCi; specific activity, 2.15 mCi/153 µg for CH3397; administered dose, 1.43 mCi; specific activity, 1.61 mCi/179 µg for RH600)

Organ-animal ID	cpm/g (× 10⁶)	cpm/CD4⁺ (× 10⁻³)	cpm/CD4⁻ (× 10⁻³)	No. of CD4⁺ cells/g (× 10⁹)* (RD)	No. of lymphocytes/g† (× 10⁹) (TCE)	Percentage of CD4⁺ T cells	No. of lymphocytes/g‡ (× 10⁹) (RD + FC)	Ratio§
Spleen-CH3397	4.98	3.65	0.51	1.36	4.87	NA	3.40	7.0
Axillary LN-CH3397	9.83	6.89	0.63	1.43	11.60	NA	4.14	3.6
Mesenteric LN-CH3397	4.54	3.53	0.23	1.29	3.84	NA	3.74	9.8
Spleen-RH600	3.18	3.11	0.33	1.02	2.75	41.8	2.44	8.9
Tonsil-RH600	3.90	1.88	0.04	2.07	5.00	29.8	6.95	13.9
Axillary LN-RH600	2.97	1.93	0.08	1.54	10.80	24.3	6.34	5.9
Inguinal LN-RH600	2.66	0.91	0.14	2.92	3.00	30.8	9.48	31.7
Mesenteric LN-RH600	1.04	0.90	0.05	1.16	1.67	45.2	2.57	15.5
Submandibular LN-RH600	3.03	1.46	0.11	2.07	8.82	45.5	4.55	5.16

RD indicates radioactivity data; TCE, tissue cell extraction; FC, flow cytometry; LN, lymph node; and NA, not applicable.

*No. of CD4⁺ cells per gram of tissue estimated from radioactivity data [(cpm/g)/(cpm/CD4⁺ cells)].

†No. of lymphocytes per gram of tissue obtained from TCE.

‡No. of lymphocytes per gram of tissue obtained from RD and FC. For the spleen and lymph nodes of the CH3397, the percentage of CD4⁺ T cells for the spleen and mean value for all lymph nodes of the RH600 were used.

§Ratio of no. of lymphocytes estimated from RD + FC vs the no. obtained from TCE.

Number of CD4⁺ lymphocytes in the body

We next used these data to estimate the total body number of CD4⁺ lymphocytes. We estimated that approximately 90% of the radioactivity measured in the excised intact lymph nodes and spleen (cpm/g) is the result of specific binding to CD4⁺ cells and the remaining 10% is the result of nonspecific uptake of the radiotracer in CD4⁻ cells in the pellets. An additional contribution to the nonspecific uptake is brought by the blood in tissues. The percentage of blood volume in the spleen has been reported to be between 20% and 40% from studies in rats[18] and humans.[19] We estimate that the blood accounts for 10% to 15% of the total radioactivity measured in one gram of spleen (using as reference the cpm/g in the spleen of CH3397 [Table 2] and the radioactivity measured in the blood of the same animal of 2.1×10^6 cpm/mL). Thus, by subtracting the aforementioned 2 contributions of nonspecific uptake (between 20% and 25%), we estimate approximately 1.1×10^9 CD4⁺ cells per gram of spleen of CH3397. In extrapolating these data to humans, using the value of 1.1×10^9 CD4⁺ cells/g for the spleen of the uninfected monkey and given a mean spleen weight in a 70-kg adult human of 145 g,[20,21] one can estimate a human spleen would contain approximately 1.6×10^{11} CD4⁺ cells. Using a value of 30% for the fraction of splenic lymphocytes that are CD4⁺ cells,[21] one can calculate that the entire human spleen contains approximately 5.3×10^{11} lymphocytes. Assuming that the spleen contains approximately 15% of the total lymphoid pool,[1,22] we calculate the total body number of lymphocytes to be approximately 3.5×10^{12}, or approximately 8-fold higher than previously reported.[1,2,22] To attempt to validate these estimates derived from in vivo labeling with the anti-CD4 antibody, we calculated the number of lymphocytes present in the spleen and lymph nodes of the uninfected monkey CH3397 through cell counting analysis of sections of immunohistochemistry stained tissue sections (supplemental data). By these methods, we calculate a lower estimate for the total number of lymphocytes in the spleen to be 2.9×10^{11} and, by extrapolation, the total body number of lymphocytes in humans to be 1.9×10^{12} or approximately 4-fold higher than previously reported. One implication of these estimates is that, in a healthy subject, the lymphocytes in the blood contribute substantially less to the total lymphocyte pool than the frequently cited 2% value.[1,2,22] If one assumes a total blood volume of 5 L in a 70-kg adult human, a peripheral blood lymphocyte count of 2000 cells/µL, and that 50% of these cells are CD4⁺ T cells, the total number of lymphocytes in the blood would be calculated to be 10×10^9,[1] and the number of CD4⁺ T cells 5×10^9. Given the aforementioned range of 1.9×10^{12} to 3.5×10^{12} lymphocytes in the body, the blood would contribute between 0.3% and 0.5% to the total pool of lymphocytes.

Discussion

The present study has demonstrated that one can perform total body imaging of the CD4 pool in vivo and use this approach to observe differences at different phases of lentiviral infection. Using this technique, we were able to determine that the relationship between the CD4 pool in the lymphoid tissues and the peripheral blood is governed by an exponential law and that the total number of lymphocytes in adult humans is probably 4- to 8-fold higher than previously estimated.

Clinical decisions for HIV-1–infected patients, including starting an antiretroviral regimen or switching to a new antiretroviral

regimen, are mainly based on the CD4 T-cell counts (the main targets of HIV infection) in the blood. This compartment has been reported to represent approximately 2% of total body lymphocytes.[1,2,22] The CD4 T-cell count in the blood is recognized as a major prognostic marker of disease progression. Despite the critical role of CD4+ T cells in host defense, the peripheral blood CD4+ T-cell count appears to predict only up to 30% of the variability in AIDS or death for all causes.[3] One possible explanation is that the true changes in total body CD4 cells are not well reflected by this measurement. Reasons for this include variability resulting from trafficking and tissue distribution.[23,24] The rationale for this study was to generate a more comprehensive picture of the CD4 pool in the entire body in nonhuman primates in the settings of lentiviral infection.

The noninvasive imaging technique to monitor CD4 T-cell numbers throughout the body described here requires the administration of small amounts of a humanized nondepleting mAb ($\sim$ 20 μg/kg), approximately 500-fold lower than the dose administered to induce immunosuppression in monkeys who received a renal allograft.[25] In our study, we have shown that this radiotracer is able to detect differential levels of CD4 cells in lymphoid organs of nonhuman primates characterized by differential levels of CD4 T-cell counts in the peripheral blood. We observed that the relationship between the radiotracer retention in lymphoid organs and the number of CD4+ T cells per unit volume of blood was governed by an exponential law, not a linear law. This nonlinearity most probably arises as a consequence of changes in the equilibrium/distribution of CD4+ T cells between peripheral blood and lymphoid organs at different peripheral blood CD4 counts during infection. This interpretation is consistent with previous observations in simian immunodeficiency virus-infected monkeys in which more dramatic decreases in the CD4 pool of lymph nodes have been reported to occur when the CD4 T-cell count in the peripheral blood falls below 200 to 300 CD4+ T cells/μL.[26] The nonlinearity may also arise as differential binding of the tracer between animals characterized by differential densities of CD4 receptors in the lymphoid organs or differential concentrations of the tracer. Further studies are required to address the precise origin of this relationship.

From radioactivity data of extracted tissues, we found that the number of CD4+ cells per unit gram of spleen or lymph nodes is approximately 10^9, an estimate that is approximately one order of magnitude higher than that obtained from procedures of cell extraction followed by flow-cytometric analysis. This would also be consistent with the density of lymphocytes measured from analysis of immunohistochemistry stained spleen tissue sections. One possible explanation for this discrepancy is that the procedure of extraction leads to an underestimate of the true number of cells per unit gram of tissue resulting from the loss of cells during the mechanical disruption of tissues, washing procedures, and pelleting, whereas measurements of radioactivity data are performed on intact tissues. The estimate generated from the radioactivity data are approximately 2-fold higher than the estimate generated from the tissue section analysis. This discrepancy may be the result of the variance introduced by sampling errors of the excised organs or the assumptions used to extract quantitative information from the 2 different methodologies. The radioactivity counting technique may have generated an upper estimate of the true number of lymphocytes resulting from the possible contribution to the total radioactivity brought by additional specific or nonspecific binding of the tracer to cells not directly recovered in the tissue cell extractions, including macrophages or Fc receptor-bearing cell populations. However, the number of CD4 receptors in macrophages has been reported to be low,[27,28] and human IgG4 has been reported to have low binding for the high affinity Fc gamma receptor, FcγRI receptor.[29] The tissue section analysis may have generated a lower estimate because of the assumption of optimal efficiency of staining.

Given the previously reported estimate of 4 to 5×10^{11} total body lymphocytes in adult humans[22] and our observation of approximately 4- to 8-fold more lymphocytes per gram of lymphoid tissues from our radioactivity data, we propose that the total number of lymphocytes in humans is approximately 1.9 to 2.9×10^{12}.

SPECT imaging or direct radioactivity measurements of any subcompartment (jejunum, ileum, ascending and descending colon) of the small and large intestine did not reveal differences between high and low CD4 T-cell counts, thus suggesting that the number of photons elicited per unit volume (mass) in these organs was the result of radioactive background activity. We observed that each gram of spleen carried at least 10-fold more CD4 cells than each gram of gut in an uninfected monkey. Given that the weight of the spleen (145 g)[20,21] is approximately 10-fold lower than the weight of the total gut in adult humans (1100-1500 g),[30] it can be concluded that at the most the gut contains a number of CD4+ T cells equal to that of the spleen. Because the relative contribution of the spleen to the entire pool of lymphocytes is approximately 15%,[1,21] then an upper limit for the relative contribution of the gut to the entire pool of lymphocytes should also be approximately 15%. The lower density of lymphocytes in the small and large intestines compared with lymph nodes and spleen is in part explained by the characteristic high heterogeneity of gut tissues where the majority of mass is occupied by muscularis externa and submucosa compartments, which harbor a negligible amount of lymphocytes in between fat layers (supplemental Figure 3). Our results are consistent with the previously reported low number of total lymphocytes per gram of gut in adult pigs,[31] rhesus monkeys,[32] and humans,[2,33,34] as recently reviewed by Ganusov and De Boer.[22]

Taken together, these data suggest a need to reevaluate current assumptions regarding the relative contribution of different tissues to the overall pool of CD4+ T cells. Using SPECT and monoclonal antibody imaging, we were able to visualize only relatively large clusters of lymph nodes and the spleen; nevertheless, a significant portion of the lymphoid organs compared with the blood compartment. By combining the data from in vivo imaging with ex vivo images of isolated organs and gamma counter analysis of tissue fragments, we feel the data here extend the precision of estimates regarding the relative numbers of CD4 T cells in different organs. CD4-binding tracers characterized by faster biodistribution in the body coupled with imaging platforms characterized by higher spatial resolutions (eg, positron emission tomography) and CT scans for a precise volumetric analysis of the regions of interest might increase the portion of lymphoid tissue that could be visualized in the whole body noninvasively. The ability to accurately assess the state of the total body CD4+ T-cell pool from total body imaging may provide a better understanding of the relationships between different physiologic and pathophysiologic states and CD4+ T-cell distribution, depletion, and reconstitution.

Acknowledgments

Authorship

Contribution: M.D.M. designed and performed research, analyzed/interpreted the data, made the figures, and wrote the paper; C.H.P. designed and performed research, analyzed/interpreted the data, and critically reviewed the paper; J.A.C. designed research, analyzed/interpreted the data, and critically reviewed the paper; J.-S.M. performed research and analyzed the data; B.-S.J. performed research, analyzed the data, and critically reviewed the paper; I.S.S. performed research and analyzed the data; S.S. performed research, analyzed/interpreted the data, made the figures, and critically reviewed the paper; R.B. performed research and critically reviewed the paper; A.N. and W.K. performed research; M.C. performed research and critically reviewed the paper; Y.N., K.R., and M.M. designed research and critically reviewed the paper; and H.C.L. designed research, analyzed/interpreted the data, and critically reviewed the paper.

Conflict-of-interest disclosure: The authors declare no competing financial interests.

Correspondence: Michele Di Mascio, NIAID, NIH, 6700A Rockledge Dr, Rm 5232, Bethesda, MD 20817; e-mail: mdimascio@niaid.nih.gov.

References

1. Westermann J, Pabst R. Distribution of lymphocyte subsets and natural killer cells in the human body. *Clin Invest.* 1992;70:539-544.

2. Trepel F. Number and distribution of lymphocytes in man: a critical analysis. *Klin Wochenschr.* 1974;52:511-515.

3. Mellors JW, Margolick JB, Phair JP, et al. Prognostic value of HIV-1 RNA, CD4 cell count, and CD4 cell count slope for progression to AIDS and death in untreated HIV-1 infection. *JAMA.* 2007;297:2349-2350.

4. Rubin RH, Baltimore D, Chen BK, Wilkinson RA, Fischman AJ. In vivo tissue distribution of CD4 lymphocytes in mice determined by radioimmunoscintigraphy with an 111In-labeled anti-CD4 monoclonal antibody. *Proc Natl Acad Sci U S A.* 1996;93:7460-7463.

5. Delmonico FL, Knowles RW, Colvin RB, et al. Immunosuppression of cynomolgus renal allograft recipients with humanized OKT4A monoclonal antibodies. *Transplant Proc.* 1993;25:784-785.

6. Kinuya S, Jeong JM, Garmestani K, et al. Effect of metabolism on retention of indium-111-labeled monoclonal antibody in liver and blood. *J Nucl Med.* 1994;35:1851-1857.

7. Camera L, Kinuya S, Garmestani K, et al. Evaluation of a new DTPA-derivative chelator: comparative biodistribution and imaging studies of 111In-labeled B3 monoclonal antibody in athymic mice bearing human epidermoid carcinoma xenografts. *Nucl Med Biol.* 1993;20:955-962.

8. Abaza MS, Atassi MZ. Effects of amino acid substitutions outside an antigenic site on protein binding to monoclonal antibodies of predetermined specificity obtained by peptide immunization: demonstration with region 94-100 (antigenic site 3) of myoglobin. *J Protein Chem.* 1992;11:433-444.

9. Lindmo T, Bunn PA Jr. Determination of the true immunoreactive fraction of monoclonal antibodies after radiolabeling. *Methods Enzymol.* 1986;121:678-691.

10. Pardridge WM, Eisenberg J, Yamada T. Rapid sequestration and degradation of somatostatin analogues by isolated brain microvessels. *J Neurochem.* 1985;44:1178-1184.

11. Yao Z, Garmestani K, Wong KJ, et al. Comparative cellular catabolism and retention of astatine-, bismuth-, and lead-radiolabeled internalizing monoclonal antibody. *J Nucl Med.* 2001;42:1538-1544.

12. Earl PL, Americo JL, Wyatt LS, et al. Recombinant modified vaccinia virus Ankara provides durable protection against disease caused by an immunodeficiency virus as well as long-term immunity to an orthopoxvirus in a non-human primate. *Virology.* 2007;366:84-97.

13. Department of Health and Human Services. Animals. In: *Guide for the Care and Use of Laboratory Animals* [National Institutes of Health 85-23]. Washington, DC: Department of Health and Human Services; 1985.

14. Witzig TE, Gordon LI, Cabanillas F, et al. Randomized controlled trial of yttrium-90-labeled ibritumomab tiuxetan radioimmunotherapy versus rituximab immunotherapy for patients with relapsed or refractory low-grade, follicular, or transformed B-cell non-Hodgkin's lymphoma. *J Clin Oncol.* 2002;20:2453-2463.

15. Liu Y, Wu C. Radiolabeling of monoclonal antibodies with metal chelates. *Pure Appl Chem.* 1991;63:427-463.

16. Kanwar B, Gao DW, Hwang AB, et al. In vivo imaging of mucosal CD4(+) T cells using single photon emission computed tomography in a murine model of colitis. *J Immunol Methods.* 2008;329:21-30.

17. Zamarchi R, Ranozzo M, Del Mistro A, et al. B and T cell function parameters during zidovudine treatment of human immunodeficiency virus-infected patients. *J Infect Dis.* 1994;170:1148-1156.

18. Sebestík V, Brabec V. Red cell, plasma and whole blood volumes in organs of normal and hypersplenic rats. *Blut.* 1974;29:203-209.

19. Leggett RW, Williams LR. Suggested reference values for regional blood volumes in humans. *Health Phys.* 1991;60:139-154.

20. Hellman T. Die Altersanatomie der menschlichen Milz. Studien besonders uber die Ausbildung des lymphoiden Gewebes und der Sekundarknotchen in verschiedenen. Vol. 12. Lehre: Altern Z Konstit; 1926.

21. Krumbhaar EB, Lippincott SW. Postmortem weight of "normal" human spleens at different ages. *Am J Med Sci.* 1939;197:344-358.

22. Ganusov VV, De Boer RJ. Do most lymphocytes in humans really reside in the gut? *Trends Immunol.* 2007;28:514-518.

23. Autran B, Carcelain G, Li TS, et al. Positive effects of combined antiretroviral therapy on CD4+ T cell homeostasis and function in advanced HIV disease. *Science.* 1997;277:112-116.

24. Pakker NG, Notermans DW, de Boer RJ, et al. Biphasic kinetics of peripheral blood T cells after triple combination therapy in HIV-1 infection: a composite of redistribution and proliferation. *Nat Med.* 1998;4:208-214.

25. Mourad GJ, Preffer FI, Wee SL, et al. Humanized IgG1 and IgG4 anti-CD4 monoclonal antibodies: effects on lymphocytes in the blood, lymph nodes, and renal allografts in cynomolgus monkeys. *Transplantation.* 1998;65:632-641.

26. Rosenberg YJ, Shafferman A, White BD, et al. Variation in the CD4+ and CD8+ populations in lymph nodes does not reflect that in the blood during SIVMNE/E11S infection of macaques. *J Med Primatol.* 1992;21:131-137.

27. Lewin SR, Sonza S, Irving LB, McDonald CF, Mills J, Crowe SM. Surface CD4 is critical to in vitro HIV infection of human alveolar macrophages. *AIDS Res Hum Retroviruses.* 1996;12:877-883.

28. Thomas ER, Dunfee RL, Stanton J, et al. Macrophage entry mediated by HIV Envs from brain and lymphoid tissues is determined by the capacity to use low CD4 levels and overall efficiency of fusion. *Virology.* 2007;360:105-119.

29. Canfield SM, Morrison SL. The binding affinity of human IgG for its high affinity Fc receptor is determined by multiple amino acids in the CH2 domain and is modulated by the hinge region. *J Exp Med.* 1991;173:1483-1491.

30. International Commission on Radiological Protection. Report of the Task Group on Reference Man. Vol. 23. International Commission on Radiological Protection; 1975.

31. Rothkötter HJ, Kirchhoff T, Pabst R. Lymphoid and non-lymphoid cells in the epithelium and lamina propria of intestinal mucosa of pigs. *Gut.* 1994;35:1582-1589.

32. Sopper S, Nierwetberg D, Halbach A, et al. Impact of simian immunodeficiency virus (SIV) infection on lymphocyte numbers and T-cell turnover in different organs of rhesus monkeys. *Blood.* 2003;101:1213-1219.

33. Bull DM, Bookman MA. Isolation and functional characterization of human intestinal mucosal lymphoid cells. *J Clin Invest.* 1977;59:966-974.

34. Selby WS, Janossy G, Bofill M, Jewell DP. Intestinal lymphocyte subpopulations in inflammatory bowel disease: an analysis by immunohistologic and cell isolation techniques. *Gut.* 1984;25:32-40.